Thinking about metal-metal quadruple bonding in extended structures: a hypothetical $A_2M_6E_8$ network

Musiri M. Balakrishnarajan,[a] Peter Kroll,[b] Michael J. Bucknum[a] and Roald Hoffmann*[a]

[a] Department of Chemistry and Chemical Biology, Baker Laboratory, Cornell University, Ithaca, NY 14853-1301, USA. E-mail: rh34@cornell.edu

[b] Institut für Anorganische Chemie, Rheinisch-Westfälische Technische Hochschule Aachen, Professor-Pirlet-Strasse 1, 52056, Aachen, Germany

The electronic and structural possibilities of a recently conceived, as-yet unsynthesized, AM_6E_8 (or $A_2M_6E_8$) structural type are explored. With A an alkaline earth metal, M a transition metal, and E a main group element, a range of geometries containing M–M pairs with very short separations is feasible. Density functional theory geometry optimizations and an extended Hückel analysis of the bonding in a representative $Ca_2W_6O_8$ realization support the qualitative picture of quadruple metal-metal bonding in these hypothetical phases. The MM pairs interact moderately (metallic behavior is anticipated) through linking atoms. Geometry optimizations of a wide range of hypothetical compounds show that the M–M separation in these will be in the range of realistic quadruple metal-metal bonding, 2.20–2.30 Å.

The working out of the idea of metal-metal quadruple bonding by F. A. Cotton is certainly one of the prettiest chapters of modern chemistry.[1] Can one realize such bonding in extended structures? There are a number of compounds in which short metal-metal separations are observed and which reach formal bond orders of three—for instance, RE_2ReO_5 (RE = rare earth),[2] $RE_3Re_2O_9$,[2] $Li_6Ca_2Mn_2N_6$,[3] $Ca_6Cr_2N_6H$,[4] $NaNb_3O_5F$,[5a] $Ca_{0.75}Nb_3O_6$,[5b] $Ca_{0.95}NbO_6$,[5c] $Na_{0.74}Ta_3O_6$[5d] and some others.[6] Here we propose a hypothetical three-dimensional network that, while apparently not yet made, seems attainable and that should allow moderately localized MM quadruple bonds.

The structure

One of us (MJB) recently proposed a new AM_6E_8 network, space group $Pm3$.[7] The network is shown in Fig. 1. The atoms are located as follows: A: 1(a) (0, 0, 0); M: 6(f) $\pm$(x, 0, 1/2); E: 8(i) $\pm$(y, y, y). This net may also exist as a centered $A_2M_6E_8$ variant, with an additional A atom at (1/2, 1/2, 1/2).

There are several possibilities to relate the proposed $A_2M_6E_8$ structure to well-known structural types in solid state chemistry. The closest connection is to the known Pt_3O_4 structure and the Pt bronzes and their chalcogenide analogs.[8] In these the Pt–Pt bonding is weak (and interesting) and linearly extended, which, as we will see, is a point of contrast to the structures we propose.
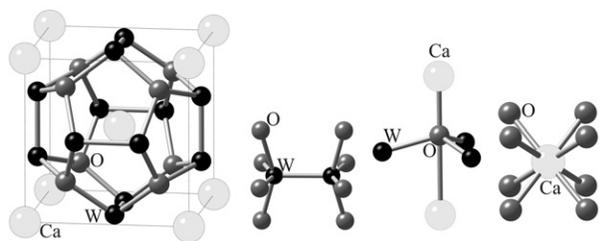
Another connection may be made to the Cr_3Si type (A15 in *Strukturberichte*). The A_2M_6 (=M_3A=Cr_3Si) framework is stuffed with eight E atoms that fill trigonal bypyramidal holes. The superconducting Nb_3Ge and Nb_3Sn phases belong to this structural family too.[9a] Our particular choice of atoms A, M, and E can be thought of as causing bond localization within the chains formed by the M atoms of the above-mentioned structures.[9b]

The $A_2M_6E_8$ structure may also be related to the fluorite structure type (CaF_2). In CaF_2, Ca atoms are arranged in a cubic closest packing (ccp) arrangement, forming a face-centered cell with Ca atoms at the origin as well as on the faces of the cube. F atoms occupy all tetrahedral holes. The coordination of Ca is eight, that of F is four. The octahedral interstitial sites (in the center of the cell as well as on the edges) are empty. The composition of the conventional cubic unit cell of CaF_2 is Ca_4F_8. $A_2M_6E_8$ can be derived from CaF_2 in the following way: the Ca at the origin is replaced by an A atom. Then we split every Ca on the faces into an M–M dimer and exchange all F by E atoms. Finally, we fill the octahedral site in the center of the cube with one A.

We present these relations to known structural types because of their potential utility in the design of a manifold of structures containing dimer pairs.

Design, potential realizations, and sample calculations

Putting A = an alkaline earth metal (a lanthanide, actinide or alkali metal would fit as well), M, a transition metal, and E, a main group element from group 15, 16, or 17, we found a large range of viable structures. Viable is in the sense of A–E, A–M falling in the range of normal ionic separations, M–E a typical coordinate covalent distance, and M–M short, in the range of MM multiple bonds. The environment of the MM unit in AM_6E_8 is clearly approximately that of $Re_2Cl_8^{2-}$, as Fig. 1 shows.

A further exploration began with three representative d^4–d^4 compounds: $Ca_2W_6O_8$, $CaNb_6Cl_8$, and $La_2Re_6N_8$. When computed within the extended Hückel (eH) method, the first

Fig. 1 The proposed $A_2M_6E_8$ structure.

of these had a reasonable gap between three flattish δ bonding bands and three δ* antibonding ones. The other two compounds were metallic as a result of greater dispersion due to A–E and M–E interactions.

When $Ca_2W_6O_8$ was calculated with the Vienna *Ab initio* Simulation Package (VASP) density functional theory (DFT) suite of programs (see details in the Theoretical methods section), permitting complete optimization of all structural parameters (atomic positions and the lattice constant), there resulted a short W–W distance of 2.27 Å. The distance is similar to WW quadruple bond separations in molecular solids, for example, 2.165 Å in $W_2(O_2CR)_4$ and 2.26 Å in $Li_4W_2(CH_3)_xCl_{8-x}$·THF and $Li_4W_2(CH_3)_8$.[10]

There is an important difference between the eH and DFT results for $Ca_2W_6O_8$. In the latter there was substantive density of states (DOS) and band crossing at the Fermi level region. The disagreement led us in two directions: (a) exploration with the more reliable DFT code of a wider range of compounds and (b) a readjustment of the eH parameters, so as to potentially match the DFT results.

Table 1 shows the compounds we studied, in each case optimizing all structural parameters. Most are d^4 systems (88 electrons in the formula unit), but we also included a range of compounds with formal electron counts ranging from $d^{2.67}$ to $d^{4.67}$. Clearly atom substitutions can be used to tune the electron count and to study its influence on the structure, in particular the W–W bond distance. What is remarkable is how stable the short W–W distance is in these compounds. It is down to 2.08 Å in one case, up to 2.37 Å in another, but mostly stays in the quadruple bond range of 2.20–2.30 Å. The shortest WW bond is obtained for 88 electrons, the d^4–d^4 system. There is no correlation of WW distances with the lattice constant. We take the computed geometries as an indication that these systems should be stable. All systems turn out to be metallic in the DFT calculations, except $W_6E_8^{4-}$, E = O, S, and $W_6O_4F_4$ (no A atom in these cases).

Our parallel efforts to reparameterize the eH method, driven by the multitude of analytical tools available within this method, focused on a still more hypothetical (countercation-free) $W_6O_8^{4-}$ and $Ca_2W_6O_8$. A change of 2 eV in the H_{ii} of W 5d, and a small adjustment in the diffuseness of the W 5d orbital (the final eH parameters are given in the Theoretical methods section) gave band structures for $W_6O_8^{4-}$ similar to the DFT results. Some further small variation in the

parameters produced a reasonable correspondence between the eH and DFT band structures of $Ca_2W_6O_8$. With the new parameters, the $Ca_2W_6O_8$ system is metallic in eH.

Metal–metal bonding in molecules and the extended structures

Though the W–W distances computed in our systems are certainly short, is there in fact WW quadruple bonding in these structures? Let us look first at a model d^4–d^4 molecular system, $W_2O_8^{12-}$, computed in the geometry that a dimer unit has in $Ca_2W_6O_8$. Fig. 2 shows a construction of such a molecule, from two WO_4^{6-} units. Nothing surprising here—we see the expected pattern[1] of σ, π, δ, δ*, π*, σ* levels as one goes up in energy, perturbed only by an inversion in the order of the π* and σ* levels.

Fig. 3 compares local σ, π, and δ contributions to the W–W crystal orbital overlap population (COOP) in $W_6O_8^{4-}$ and $Ca_2W_6O_8$. Each was calculated within the eH method, using DFT optimized geometries and the adjusted eH parameters mentioned. σ, π and δ refer to all combinations that contribute to the COOP, so for instance π is not only $d_{xz}(1) - d_{xz}(2)$ but also includes $d_{xz}(1) + p_x(2)$ and $p_x(1) + p_x(2)$ contributions (where z is the internuclear axis; obviously the analysis is restricted to one of the three equivalent W_2 sets).

$W_6O_8^{4-}$ has a band gap, $Ca_2W_6O_8$ does not. We see in both compounds well-defined σ, π, δ, δ*, π*, σ* regions, though not necessarily in that order. The Fermi level for $W_6O_8^{4-}$ comes exactly at the crossing of the W–W COOP from bonding to antibonding, and not far from that crossing in $Ca_2W_6O_8$. In the latter compound there is some electron transfer from the $W_6O_8^{4-}$ sublattice to the Ca^{2+} sublattice; this moves the Fermi level into the δ region of the metal oxide sublattice. A crystal orbital Hamilton population (COHP) analysis of the DFT calculation on $Ca_2W_6O_8$ leads to the same conclusion.

Band structure

The band structure of $Ca_2W_6O_8$ is shown in Fig. 4 together with the DOS. $Ca_2W_6O_8$ turns out to be metallic. From the DOS in Fig. 4 we see that the whole region around the Fermi level is made up from W d electrons, with a small admixture of O p electrons. There is a pseudo-gap at about $E = -1.4$ eV. Interestingly, the DOS shows several pronounced peaks, for example one at -1.9 eV below the Fermi level. This peak

Table 1 Computed crystal structure data for $A_2W_6E_8$ compounds. Ne^-: number of electrons in the formula unit; a is the lattice constant; x_W: x coordinate of the W atom; y_{E1}: y coordinate of the E1 atom; y_{E2}: y coordinate of the $E2$ atom (only for structures with two kinds of anions E); d_{W-W}: W–W bond distance; d_{W-E1}: W–E1 bond distance; d_{W-E2}: W–E2 bond distance; d_{A1-E}: distance A1 (at corner of the unit cell) to E; d_{A2-E}: distance A2 (at center of the unit cell) to E. All distances are in Å.

| Composition	Space group	Ne⁻	a	x_W	y_{E1}	y_{E2}	d_{W-W}	d_{W-E1}	d_{W-E2}	d_{A1-E}	d_{A2-E}
$W_6O_8^{4-}$	Pm-3	88	6.513	0.330	0.265	–	2.22	2.35	–	2.65	2.99
$W_6S_8^{4-}$	Pm-3	88	7.486	0.351	0.267	–	2.23	2.73	–	3.02	3.47
$W_6S_4P_4$	$P23$	80	6.743	0.329	0.257	0.741	2.31	2.43	2.43	–	–
$W_6O_4Cl_4$	$P23$	88	6.168	0.322	0.277	0.799	2.19	2.21	2.35	–	–
$W_6O_4N_4$	$P23$	80	5.698	0.292	0.259	0.755	2.37	2.03	2.03	–	–
$W_6O_4F_4$	$P23$	88	5.878	0.316	0.262	0.731	2.16	2.11	2.10	–	–
$W_6S_4Cl_4$	$P23$	88	6.776	0.337	0.257	0.737	2.20	2.46	2.45	–	–
W_6Cl_8	Pm-3	92	6.837	0.337	0.259	–	2.22	2.48	–	–	–
W_6S_8	Pm-3	84	6.719	0.331	0.260	–	2.28	2.42	–	–	–
$Ca_2W_6S_8$	Pm-3	88	6.818	0.337	0.253	–	2.22	2.48	–	2.99	2.91
$Mg_2W_6S_8$	Pm-3	88	6.765	0.337	0.252	–	2.21	2.46	–	2.95	2.91
$K_2W_6S_8$	Pm-3	86	6.865	0.336	0.257	–	2.26	2.49	–	3.05	2.89
W_6O_8	Pm-3	84	5.725	0.304	0.254	–	2.24	2.04	–	–	–
W_6F_8	Pm-3	92	6.034	0.327	0.233	–	2.08	2.21	–	–	–
$Be_2W_6O_8$	Pm-3	88	5.668	0.303	0.214	–	2.24	2.09	–	2.10	2.81
$Mg_2W_6O_8$	$Pm\,3$	88	5.780	0.307	0.225	–	2.23	2.11	–	2.25	2.75
$Ca_2W_6O_8$	$Pm\,3$	88	5.879	0.307	0.251	–	2.27	2.10	–	2.56	2.53
$Zn_2W_6O_8$	$Pm\,3$	88	5.777	0.307	0.225	–	2.23	2.11	–	2.25	2.75
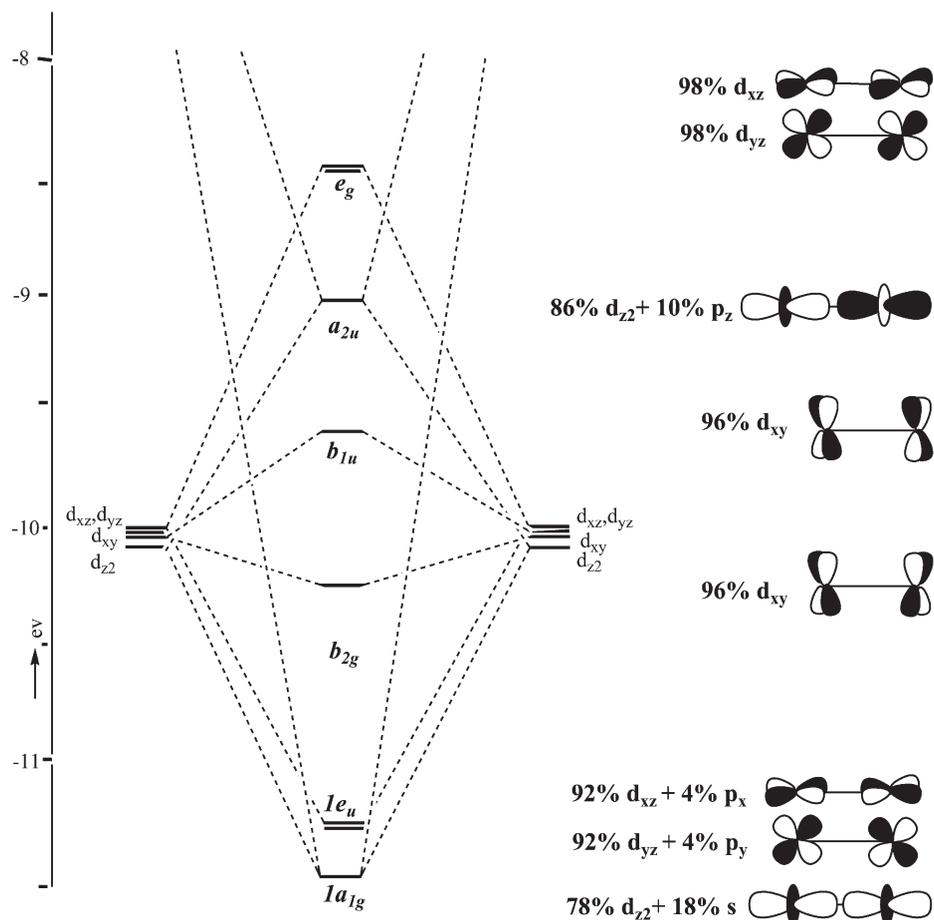
Fig. 2 Interaction of two WO_4^{6-} (C_{4v}) fragments, resulting in $W_2O_8^{12-}$ (D_{4h}). The energies are obtained from eH calculations. The major contributions to the MOs are indicated.
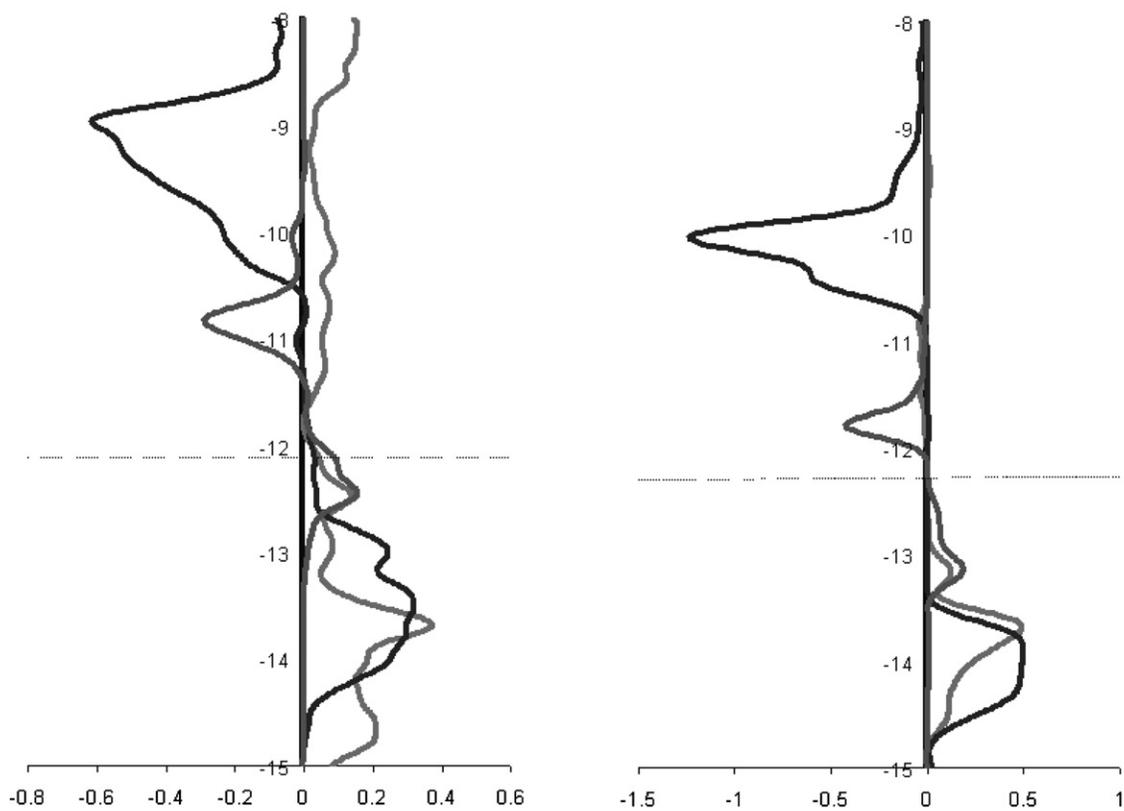

Fig. 3 Crystal orbital overlap population (COOP) between W–W in (a) $Ca_2W_6O_8$ and (b) $W_6O_8^{4-}$ as computed from eH calculations. Positive COOP indicates bonding.
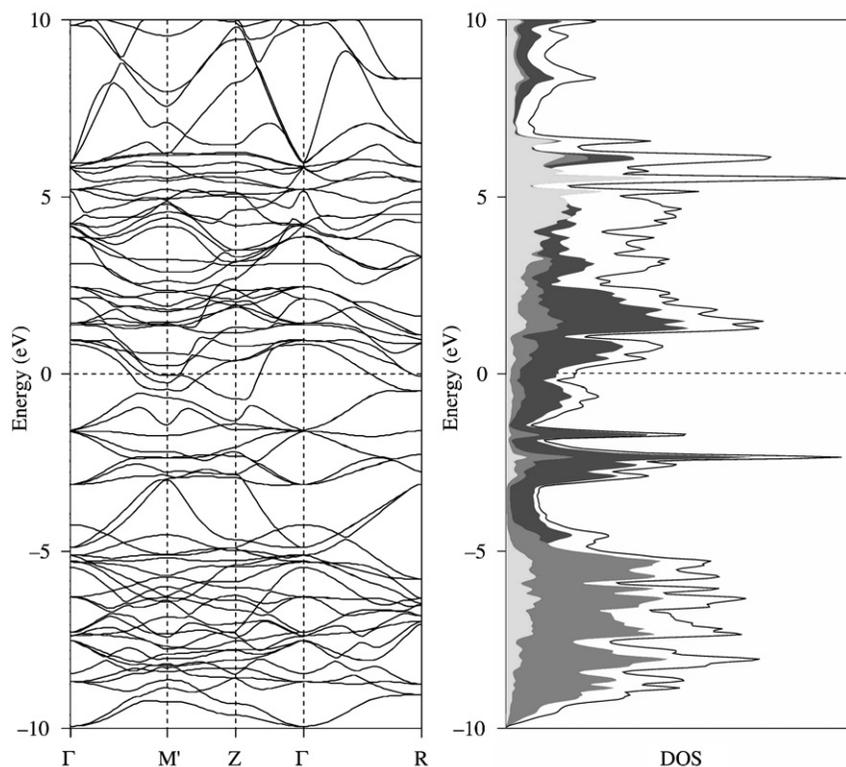
Fig. 4 Band structure of $Ca_2W_6O_8$ along lines of high symmetry in the Brillouin zone (left) and corresponding density of states (DOS; computed using a $13 \times 13 \times 13$ mesh, right). Note that we used the unconventional Z point instead of the symmetry equivalent X point. The full DOS is given by the black curve. Dark grey, medium grey and light grey filled areas show W, O, and Ca site projections of the DOS.

originates from an extremely flat band in the band structure, following the path from Γ to Z.

The Z point we use is symmetrically equivalent to the X point (so is the path Γ–Z to Γ–X). Usage of Z, however, allows the interpretation of the σ, π, and δ bands using the standard d orbitals on W. On doing so, the flat band between Γ and Z can be recognized as the δ band arising from $d_{x^2 - y^2}$ and d_{xy} orbitals on W. Steep bands are also observed, for example, the band that crosses the Fermi level between Γ and Z, which is the σ band, predominantly of d_{z^2} character. The simultaneous presence of steep and extremely flat band portions around the Fermi level has been suggested to be a "fingerprint" for a potentially superconducting compound.[11] The structural relation to the superconducting phases of Nb_3Ge and Nb_3Sn mentioned above becomes interesting in this context. One might think about removing some electrons from this material by the usual chemical stratagems, so as to bring the flat band closer to the Fermi level.

Computed COHP curves are provided in Fig. 5. The region from -10 eV to -5 eV is Ca–O and W–O bonding. The region from -5 eV to -1.6 eV is strongly W–W bonding. This strong bonding apparently dominates the structure and provides much of the cohesive energy of the system. The W–W COHP curve switches from bonding to antibonding just at the Fermi level.

Energetics

The structure of $Ca_2W_6O_8$ is mechanically stable against distortions of its structural parameters. In this sense, $Ca_2W_6O_8$ constitutes a local energy minimum on the multi-dimensional potential energy surface for this particular composition. How stable, however, might it be thermodynamically? We compared the energy of $Ca_2W_6O_8$ with the energies of its likely decomposition products, that is the enthalpy of a decomposition

reaction (at $p = 0$ Pa and $T = 0$ K). For example, $Ca_2W_6O_8$ may decompose according to the reaction:

$$Ca_2W_6O_8 \rightarrow 2CaWO_4 + 4W$$

We calculated the compounds on the right side of this reaction, scheelite and tungsten, applying the same computational procedure as for $Ca_2W_6O_8$. The enthalpy difference calculated in this way was found to be -8 eV (0.5 eV per atom).

Admittedly, this is a pretty large driving force for decomposition. There are, however, several synthetic strategies available to synthesize comparable metastable structures, such as epitaxy or template synthesis. We, therefore, think that the local minimum of this unusual structure can be attained, if not for $Ca_2W_6O_8$, then for some other realization.

Other structures with multiple metal-metal bonding

The construction principle we applied to generate the $Ca_2W_6O_8$ structure from the CaF_2 type may be applied to generate other potential extended structures with strongly bonded MM dumbbells in them. One just looks for simple structural types with at least one eight-coordinated cation, and proceeds to "split" that cation into an MM pair. For example, we may take the CsCl structure type (both Cs and Cl eight-coordinated). By splitting the central position, we come to W_2X (X any kind of anion). To make W formally 2+, X would be C with a 4$-$ formal charge.

Another opportunity is offered up by the Th_3P_4 structure type. If we split the one Th position into an M–M pair, we end up with M_3E_2, possibly quadruply bonded for M = W, E = N.[12] This formal type of crystal engineering is illustrated in Fig. 6. Interestingly, the structure we created in this way is already known in solid state chemistry, it is the anti-type of the La_2C_3 structure.[13]
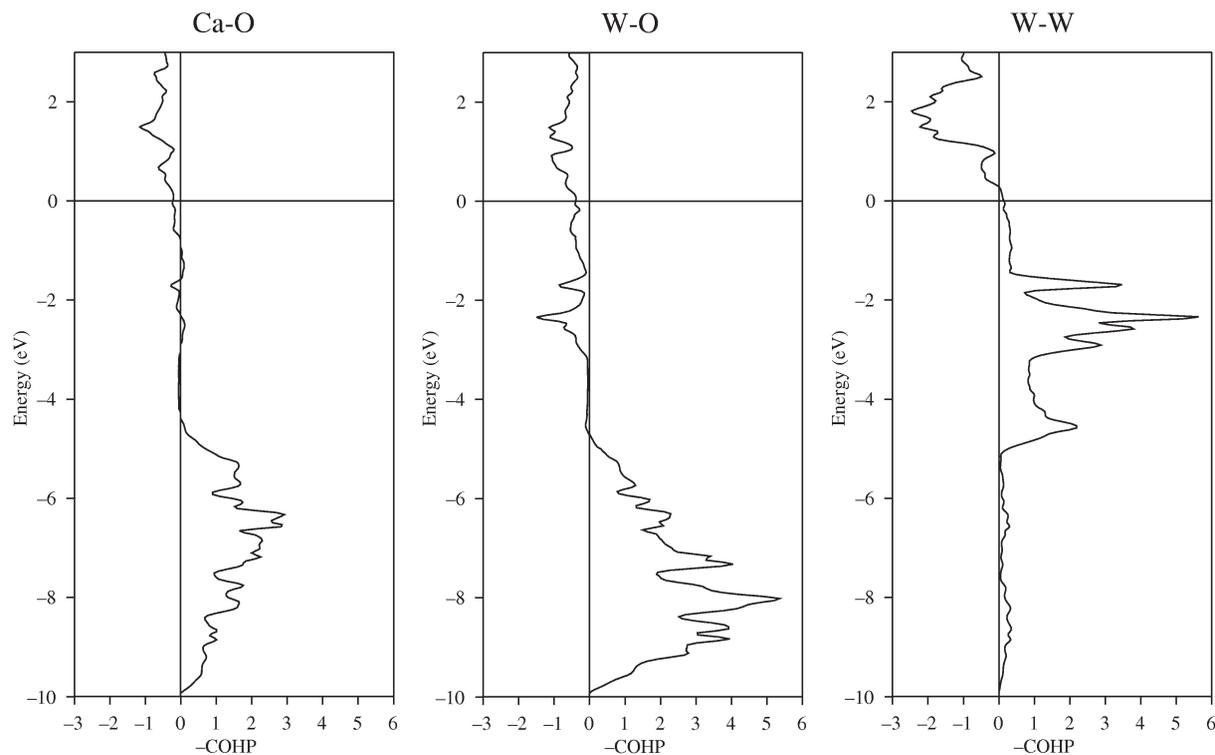
Fig. 5 COHP curves in $Ca_2W_6O_8$. Note that we plot $-COHP$, therefore, positive values (on right side of each graph) indicate bonding, negative values indicate antibonding.

In a model calculation on $W_2O_8{}^{12-}$, the D_{2d} geometry at right in Fig. 6 is destabilized (the e π levels go up in energy) relative to a D_{4h} structure. But the essential features of quadruple bonding are retained. Exploring structural stability by geometry optimization, a preliminary calculation on W_3N_2 leads (after much relaxation) to a 3-connected net (with W–W bonds). There are, however, still some large interstitial sites in this structure that could be filled with suitable atoms. Moreover, not all Th positions need to be split (there are 12 of them in the conventional unit cell of Th_3P_4).

Finally, we note that a variety of further structural types may be derived from the $A_2M_6E_8$ structure, by rotating the MM dumbbells. One highly symmetric variant (space group Pm-$3m$, Fig. 7), for instance, may be obtained by orienting the dumbbells so that they all "point" at the central site. This structure has already been studied theoretically, as a cubic alternative to the Chevrel phases.[14]

There's clearly a large playground awaiting theoretical and experimental children here.

Theoretical methods

Extended Hückel calculations were carried out using the YAeHMOP program[15] and parameters listed in Table 2. C_1,

C_2, ζ_1 and ζ_2 are the coefficients and exponents in a double-ζ expansion of the 5d Slater orbital.

For density functional calculations[16] we applied the VASP software.[17] This implementation of DFT methods combines a plane-wave basis set with the total energy pseudopotential approach. The pseudopotentials employed are based on the projector-augmented-wave (PAW) method.[18] We used both the local density approximation (LDA) and the generalized-gradient approximation (GGA) to treat the exchange-correlation energy of the electrons. All results rely on well-converged structures with respect to cut-off energy (500 eV) and k point sampling ($4 \times 4 \times 4$ mesh). Residual forces and stresses in the optimized structures are below 0.01 eV $Å^{-1}$ and 1 kbar, respectively.

We tested different kinds of pseudopotentials for Ca and W. In the case of Ca, we detected no significant difference whether the 3p electrons were treated either as core or valence states.
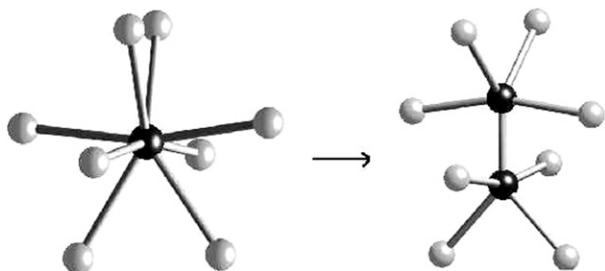

Fig. 6 A way of building up an MM multiply bonded structure by splitting of the Th position in the Th_3P_4 structure type. The regular ThP_8 bisdisphenoid is transformed into an M_2E_8 unit.
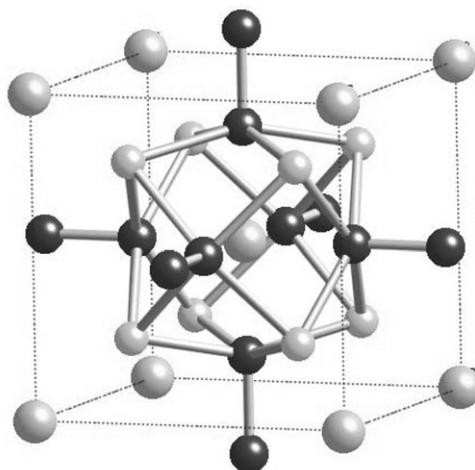
Fig. 7 A variant of the $A_2M_6X_8$ structure with higher (Pm-$3m$) symmetry.

Table 2 Extended Hückel parameters

	ζ_1	H_{ii}/eV	C_1	ζ_2	C_2
Ca 4s	1.200	−7.00			
Ca 4p	1.200	−4.00			
O 2s	2.275	−32.30			
O 2p	2.275	−14.80			
W 6s	2.340	−8.26			
W 6p	2.309	−5.17			
W 5d	4.782	−13.37	0.6685	1.860	0.5424

For W the particular choice of pseudopotential employed (defining the 5p electrons as core or valence) had no effect on the W–O bond length, but influenced the W–W bond length. Unless stated otherwise, all results reported were obtained within the GGA with pseudopotentials that have the p electrons defined as core states.

In addition we used the TB-LMTO method to analyze the electronic structure in more detail.[19] Band structure, density of states (DOS) and the crystal orbital Hamilton population (COHP)[20] were investigated within the LDA. The LMTO calculations are done for geometries first optimized within the plane-wave method.

Acknowledgements

References

1 F. A. Cotton and R. A. Walton, *Multiple Bonds between Metal Atoms*, Oxford, New York, 1993.
2 (a) W. Jeitschko, D. H. Heumannskämper, M. S. Schriewer-Pöttgen and U. Ch. Rodewald, *J. Solid State Chem.*, 1999, **147**, 218; (b) K. Waltersson, *Acta Crystallogr, Sect. B.*, 1976, **32**, 1485; (c) J.-P. Besse, G. Baud, R. Chevalier and M. Gasperin, *Acta Crystallogr., Sect. B*, 1978, **34**, 3532; (d) G. Wltschek, H. Paulus, H. Ehrenberg and H. Fuess, *J. Solid State Chem.*, 1997, **132**, 196.
3 O. Hochrein, Y. Grin and R. Kniep, *Angew. Chem., Int. Ed.*, 1998, **37**, 1582.
4 M. S. Bailey, M. N. Obrovac, E. Baillet, T. K. Reynolds, D. B. Zax and F. J. DiSalvo, *Inorg. Chem.*, 2003, **42**, 5572.
5 (a) J. Köhler and A. Simon, *Angew. Chem., Int. Ed. Engl.*, 1986, **25**, 996; (b) S. J. Hibble, A. K. Cheetham and D. F. Cox, *Inorg. Chem.*, 1987, **26**, 2389; (c) P. Alemany, V. G. Zubkov, S. Alvarez, V. P. Zhukov, V. A. Pereliaev, I. Kontsevaya and A. Tyutyunnik, *J. Solid State Chem.*, 1993, **105**, 27; (d) B. Harbrecht and A. Ritter, *Z. Anorg. Allg. Chem.*, 1999, **625**, 178.
6 For some strategies for linking large arrays of multiply-bonded MM units, see: (a) M. H. Chisholm, *J. Organomet. Chem.*, 2002, **641**, 12; (b) F. A. Cotton, C. Lin and C. A. Murillo, *Proc. Natl. Acad. Sci. U.S.A.*, 2002, **99**, 4810.
7 M. J. Bucknum, *Chemistry Preprint Server (CPS)*, 2002, physchem/0204007.
8 For leading references see: K. B. Schwartz, C. T. Prewitt, R. D. Shannon, L. M. Corliss, J. M. Hastings and B. L. Chamberland, *Acta Crystallogr. Sect. B*, 1982, **38**, 363; D. A. Keszler and J. A. Ibers, *Inorg. Chem.*, 1983, **22**, 3367; M. Wakeshima, T. Fujino, N. Sato, K. Yamada and H. Matsuda, *J. Solid State Chem.*, 1997, **129**, 1.
9 (a) J. Müller, *Rep. Prog. Phys.*, 1980, **43**, 641; L. R. Testardi, *Rev. Mod. Phys.*, 1975, **47**, 637; (b) Though it's an important and interesting topic, a detailed investigation of this Peierls distortion is out of place here.
10 A. R. Chakravarty, F. A. Cotton and E. S. Shamshoum, *Inorg. Chem.*, 1984, **23**, 4216.
11 A. Simon, *Angew. Chem., Int. Ed. Engl.*, 1997, **36**, 1788.
12 More precisely, here is what was done: Th$_3$P$_4$ is in space group *I*-43d. The cell constant was chosen as a = 8.6 Å. The Th are at 12a (3/8 0 1/4), P at 16c (x x x), with x = 1/12, which makes all Th–P distances equal, Th–P = 2.977 Å (for a = 8.6 Å). The Th position at 12a was then split into two. It becomes 24d. There is now a new free parameter, the x position of the cation (Th or W). It will determine the bond distance W–W. In the new structure the atom positions are as follows: W 24d [x(W) 0 1/4]; choose x(W) = 0.25 for W–W = 2.15 Å, N 16c (x x x); choose x = 0.0417 to have four equal bond distances W–N = 2.559 Å.
13 M. Atoji, K. A. Gschneidner, A. H. Daane, R. E. Rundle and F. H. Spedding, *J. Am. Chem. Soc.*, 1958, **80**, 1804.
14 T. Hughbanks, *Inorg. Chem.*, 1986, **25**, 1492.
15 G. A. Landrum and W. V. Glassey, *YAeHMOP: Yet Another Extended Hückel Molecular Orbital Package*, version 3.0.2. The YAeHMOP software is freely available on the web at http://sourceforge.net/projects/yaehmop/.
16 P. Hohenberg and W. Kohn, *Phys. Rev. A*, 1964, **136**, 864.
17 (a) G. Kresse and J. Hafner, *Phys. Rev. B*, 1993, **47**, 558; (b) G. Kresse and J. Hafner, *Phys. Rev. B*, 1994, **49**, 14 251; (c) G. Kresse and J. Furthmüller, *Comput. Mater. Sci.*, 1996, **6**, 15.
18 G. Kresse and D. Joubert, *Phys. Rev. B*, 1999, **59**, 1758.
19 O. K. Andersen and O. Jepsen, *The Stuttgart TB-LMTO-ASA Program*, version 47, MPI für Festkörperforschung, Stuttgart, Germany, 2000. Available under http://www.mpi-stuttgart.mpg.de/andersen.
20 R. Dronskowski and P. E. Blöchl, *J. Phys. Chem.*, 1993, **97**, 8617.